J Appl Biomed
DOI: 10.32725/jab.2026.002
journal homepage: http://jab.zsf.jcu.cz

Journal of Applied Biomedicine

Original research article

miR-500a-3p negatively regulates SOCS2 and participates in the proliferation, glycolysis, and apoptosis of HCC cells via the JAK2/STAT5 pathway

Shan Li [1], Wei Luo [2], Wei Liu [3] *

[1] *Affiliated Hospital of Hubei University of Science and Technology, Xiantao First People's Hospital, Department of Endocrinology, Xiantao City 433000, Hubei Province, China*
[2] *Jianli People's Hospital Affiliated to China Three Gorges University, Department of Oncology, Rongcheng Town, Jianli City 433300, Hubei Province, China*
[3] *Affiliated Hospital of Hubei University of Science and Technology, Xiantao First People's Hospital, Department of Gastrointestinal Surgery, Xiantao City 433000, Hubei Province, China*

Abstract
Background: HCC is a prevalent malignant tumor globally with high mortality. MiR-500a-3p plays critical roles in tumorigenesis and tumor progression.
Methods: To evaluate miR-500a-3p's role in HCC, we first analyzed its expression and prognostic value via qRT-PCR and TCGA (Kaplan–Meier analysis). We then performed extensive *in vitro* functional studies after cell transfection (mimics, anti-miR, SOCS2 OE), measuring proliferation, migration, invasion, glycolytic parameters (glucose consumption, lactate, ECAR, ATP), and apoptosis. A target relationship with SOCS2 was predicted bioinformatically and confirmed by dual-luciferase assay. Using the JAK2/STAT5 signaling pathway inhibitor Fedratinib, the activator Erythropoietin, and transfection with si-STAT5 and oe-STAT5, the molecular mechanism of miR-500a-3p in HCC was investigated. *In vivo* experiments established tumor-bearing mouse models to evaluate the effect of miR-500a-3p on tumor growth.
Results: miR-500a-3p was significantly upregulated in HCC tissues and cells, and was associated with poor patient prognosis. The overexpression of miR-500a-3p promotes the malignant progression of HCC cells. Mechanistically, miR-500a-3p directly targeted and negatively regulated SOCS2 expression. SOCS2 expression was suppressed in HCC, with its expression abrogating miR-500a-3p-mediated oncogenicity. miR-500a-3p activated the JAK2/STAT5 pathway by inhibiting SOCS2, thereby regulating the malignant biological behaviors of HCC cells. Both SOCS2 overexpression and JAK2 inhibitor treatment could reverse the activation of the JAK2/STAT5 axis and downstream effects induced by miR-500a-3p. MiR-500a-3p promoted tumor growth in tumor-bearing mice, accompanied by SOCS2 downregulation and JAK2/STAT5 pathway activation.
Conclusion: This study reveals that miR-500a-3p promotes proliferation and glycolysis while inhibiting apoptosis of HCC cells by negatively regulating SOCS2 and activating the JAK2/STAT5 pathway.

Keywords: Apoptosis; Glycolysis; Hepatocellular carcinoma; miR-500a-3p; Proliferation; SOCS2

Highlights:
- miR-500a-3p is upregulated in HCC cells;
- miR-500a-3p promotes proliferation and glycolysis of HCC cells, while inhibiting apoptosis;
- miR-500a-3p participates in the regulation of proliferation, glycolysis, and apoptosis of HCC cells via the JAK2/STAT5 pathway by suppressing SOCS2;
- miR-500a-3p facilitates tumor growth in tumor-bearing mice.

Abbreviations:
ATP – Adenosine Triphosphate; CDYL2 – Chromodomain Y-like 2; ECAR – Extracellular Acidification Rate; ECL – Enhanced Chemiluminescence; EPO – Erythropoietin; HCC – Hepatocellular Carcinoma; JAK – Janus Kinase; miRNA – microRNA; NSCLC – Non-Small Cell Lung Cancer; SOCS – Suppressors of Cytokine Signaling; STAT – Signal Transducer and Activator of Transcription

* **Corresponding author:** Wei Liu, Affiliated Hospital of Hubei University of Science and Technology, Xiantao First People's Hospital, Department of Gastrointestinal Surgery, No. 29, Middle Section of Mianzhou Avenue, Xiantao City 433000, Hubei Province, China; e-mail: Liuwei20203@hotmail.com
http://doi.org/10.32725/jab.2025.002

Submitted: 2025-09-19 • Accepted: 2026-03-09 • Prepublished online: 2026-03-09
J Appl Biomed 24/1: 10–26 • EISSN 1214-0287 • ISSN 1214-021X

Introduction

As the predominant type of primary liver cancer, Hepatocellular carcinoma (HCC) accounts for more than 90% of cases (Sangro et al., 2021; Xia et al., 2022). Its established risk factors encompass chronic infections with HBV/HCV, excessive alcohol intake, and metabolic disorders (Ito and Nguyen, 2023). Globally, HCC presents a major public health challenge (Craig et al., 2020). The primary curative treatments – surgical resection and liver transplantation – are often inapplicable as the disease is routinely detected at advanced stage, resulting in a persistently poor prognosis (Sharma et al., 2024). Consequently, elucidating the molecular pathogenesis of HCC and discovering new therapeutic targets are critical priorities in oncology research.

The development of HCC is a multistep, multigenic process driven by the aberrant activation of oncogenes, the silencing of tumor suppressor genes, and the dysregulation of critical signaling cascades (Kouroumalis et al., 2023). A pathway of significant interest is JAK/STAT, given its pivotal role in governing fundamental cellular processes (Hu et al., 2021). Its aberrant activation is tied to pathogenesis of diverse conditions, including breast cancer, cervical cancer, atopic dermatitis, and rheumatoid arthritis (Baldini et al., 2021; Gutiérrez-Hoya and Soto-Cruz, 2020; Huang et al., 2022; Shao et al., 2021). The activation of this pathway is tightly controlled by precise negative feedback mechanisms, primarily mediated by the SOCS protein family (Sobah et al., 2021). SOCS members act as key endogenous inhibitors by either directly suppressing JAK kinase activity or competing with STAT proteins for receptor binding sites. This effectively blocks STAT phosphorylation and nuclear translocation, thereby preventing excessive signaling and preserving cellular homeostasis (Kopalli et al., 2022). In various tumors, the JAK/STAT pathway is frequently subject to persistent abnormal activation, which is often closely associated with the silencing or functional loss of SOCS family members. Among them, SOCS2 is a critical regulatory factor in cytokine signal transduction mediated by the JAK/STAT axis (Letellier and Haan, 2016). The tumor suppressor SOCS2 is often downregulated in various cancers, such as breast, lung, and pancreatic cancer (He et al., 2023; Tong et al., 2019; Wang et al., 2021). Its role in inhibiting the migration and invasion of HCC cells via suppression of JAK2/STAT5 axis has been documented (Lv et al., 2023). A critical unanswered question, however, concerns the upstream mechanisms governing this aberrant loss of SOCS2 expression in HCC, which are yet to be fully elucidated.

Research has widely uncovered the critical roles non-coding RNAs play in regulating tumorigenesis and cancer development, with microRNAs (miRNAs) being a key focus. These short, approximately 22-nucleotide-long RNAs post-transcriptionally fine-tune gene expression by binding to specific sites in the 3'UTR of their target genes. This interaction typically results in mRNA degradation or the inhibition of its translation into protein (Chen and Kim, 2024). It is well-established that miRNAs, functioning as either oncogenic drivers or tumor-suppressive agents, are deeply involved in core cancer hallmarks (Semina et al., 2021; Yousefnia, 2022). The miRNA miR-500a-3p, for instance, has been implicated in the oncogenesis of NSCLC, breast, and thyroid cancers (Kim et al., 2016; Liao et al., 2018; Xiang et al., 2023).

Recent studies have shown that miR-500a-3p can regulate the JAK3/STAT5A/STAT5B signaling pathway by targeting SOCS2 (Zhang et al., 2025). In this study, we screened and validated SOCS2 as a downstream target gene of miR-500a-3p using multiple databases, and further elucidated the mechanism by which miR-500a-3p influences HCC progression through targeting SOCS2 to modulate the JAK2/STAT5 pathway. In addition, by overexpressing SOCS2, applying inhibitors and activators of the JAK2/STAT5 pathway, and constructing si-STAT5 and oe-STAT5 cell models, we investigated from multiple perspectives the effects of SOCS2 downregulation on HCC cell proliferation, glycolysis, and apoptosis via the JAK2/STAT5 pathway. The findings of this study provide a theoretical basis for considering miR-500a-3p as a potential molecular target for HCC therapy.

Materials and methods

Clinical tissue samples

Following approval from the Ethics Committee of Xiantao First People's Hospital, Affiliated Hospital of Hubei University of Science and Technology (approval number: 2024-01A), and after obtaining written informed consent from all patients, paired HCC and adjacent non-tumor tissues were collected within 30 minutes after surgery and immediately snap-frozen in liquid nitrogen.

The study included 30 patients, comprising 21 males and 9 females, among whom 17 had stage T1–T2 disease and 13 had stage T3–T4 disease. Demographic and clinical characteristics of the patients are presented in Suppl. Table S1.

Bioinformatics analysis

Transcriptomic expression data for liver hepatocellular carcinoma (LIHC) were obtained from The Cancer Genome Atlas (TCGA) project via the Genomic Data Commons (GDC) Data Portal (https://portal.gdc.cancer.gov/) (Heath et al., 2021). RNA sequencing data (HTSeq–FPKM) and miRNA sequencing data, together with corresponding clinical information, were downloaded on May 15, 2024. After quality control, samples with incomplete survival information or missing key clinical variables (>20% missing data) were excluded. A total of 369 primary tumor samples and 49 solid tissue normal samples were included in the final analysis. FPKM values were transformed to transcripts per million (TPM) and log2-transformed for downstream analyses. Differential expression analysis was performed to compare the expression levels of miR-500a-3p (derived from miRNA-seq data) and SOCS2 (derived from mRNA expression data) between tumor and normal tissues (Ally et al., 2017). To identify potential target genes of miR-500a-3p, we used four databases – TargetScanHuman v8.0 (http://www.targetscan.org/vert_80/) (Fromm et al., 2015; McGeary et al., 2019), miRDB v6.0 (http://mirdb.org/) (Chen and Wang, 2020), miRWalk v4.0 (http://mirwalk.umm.uni-heidelberg.de/) (Sticht et al., 2018), and UALCAN (http://ualcan.path.uab.edu/, based on TCGA-LIHC data) (Chandrashekar et al., 2017, 2022) (all accessed in May 2024) – and conducted analyses as follows (Zhang et al., 2022). First, all genes predicted to be targets of has-miR-500a-3p were extracted from TargetScan, miRDB, and miRWalk. High-confidence filtering criteria were then applied, including a TargetScan context+ score percentile greater than 90%, a miRDB prediction score of at least 95, and prediction by at least three miRWalk sub-databases (such as miRanda, RNA22, and PITA) with a predicted site p value less than 0.05. For the UALCAN database, we screened genes that were significantly negatively correlated with miR-500a-3p expression based on TCGA-LIHC data (Spearman $\rho < -0.3$, adjusted $p < 0.01$). Genes that met

these stringent criteria across all four databases were then intersected.

In addition, gene expression profiling interaction analysis (GEPIA; http://gepia.cancer-pku.cn/) (Tang et al., 2017) was used to assess the association of miR-500a-3p and SOCS2 expression with patient survival outcomes. In our hospital cohort, R software (v 4.2.1) and the "stats" package (v4.2.1) were employed to analyze correlations between miR-500a-3p and clinicopathological variables. For survival analyses, the median expression level was used as the cut-off for grouping, and differences were evaluated using the log-rank test. The proportional hazards assumption and survival model construction were performed using the survival package (v.3.4-0; https://cran.r-project.org/web/packages/survival/index.html), and results were visualized with survminer (v.0.4.9) and ggplot2 (v.3.3.6) (Zhang et al., 2023b).

Cell culture and transfection

The human hepatocyte cell line (THLE-2, CC-Y1833), human HCC cell lines (HCCLM3, CC-Y1191), (Huh-7, CC-Y1280), and (MHCC97, CC-Y1613) were all purchased from Enzyme Research Biotechnology Co., Ltd. (Shanghai, China). All cells were cultured in DMEM (PM150210, Elabscience, Wuhan, China), supplemented with 10% FBS (G8003, Servicebio), and maintained in a 37 °C, 5% CO_2 incubator (Vios iDx, Thermo, Waltham, MA, USA).

The mimics-NC, mimics-miR-500a-3p, anti-NC, anti-miR-500a-3p, SOCS2 overexpression construct (SOCS2, pcDNA3.1 vector), overexpression empty vector control (Vector), si-NC, si-STAT5, oe-NC, and oe-STAT5 (pcDNA3.1 vector) used in this study were all purchased from GenePharma (Shanghai, China). Transfection was conducted using Lipofectamine 2000 as per the manufacturer's protocol. Briefly, plasmids or RNAs were complexed with the reagent for 20 min and then applied to cells in serum-free medium. After a 4 h incubation at 37 °C, the medium was replaced with fresh complete medium. Transfection efficiency was evaluated 48 h later. To further investigate the mechanism, the JAK2/STAT5 pathway inhibitor Fedratinib (0.2 μM, HY-10409, MCE) and activator Erythropoietin (EPO, 200 U/ml, HY-P73521, MCE) were employed to treat cells post-transfection.

qRT-PCR

Total RNA was isolated with TRIzol reagent and quantified spectrophotometrically. cDNA synthesis was performed using a commercial reverse transcription kit (HY-K0510A, MCE, Monmouth Junction, NJ, USA) as directed. Quantitative PCR amplification was conducted with SYBR Green qPCR Mix (TAKARA, Tokyo, Japan). The $2^{-\Delta\Delta Ct}$ method was applied to calculate relative gene expression, with normalization to β-actin (mRNA) and U6 (miRNA). The primer sequences used in this study are listed in Suppl. Table S2.

CCK-8 assay

To determine the optimal experimental concentrations of the JAK2/STAT5 pathway inhibitor (Fedratinib) and agonist (EPO), cell viability was assessed using the CCK-8 assay. HCCLM3 and MHCC97 cells were treated with varying concentrations of Fedratinib (0–10 μM) and EPO (0–4,000 U/ml) to calculate their respective IC_{50} values. Subsequently, under treatment with 0.2 μM Fedratinib or 200 U/ml EPO, cell viability was measured at 24, 48, and 72 hours. After the addition of 10 μl CCK-8 reagent (ABclonal, RM02823) to each well, and incubation for 2 hours, absorbance (OD) was measured at 450 nm, and cell viability (%) was calculated accordingly. To further evaluate the effect of STAT5 on the viability of HCC cells, OD values were measured at 24, 48, and 72 hours following transfection with si-NC, si-STAT5, oe-NC, or oe-STAT5.

Colony formation assay

HCCLM3 cells were trypsinized during exponential growth, centrifuged, and resuspended. Cells were plated at 500 cells/well in 6-well plates and cultured for 10 days. Subsequently, cells were fixed with 4% PFA for 15 min and stained with Giemsa stain (S0214, Bioss, Beijing, China) for 25 min. After air-drying, colonies were counted.

Biochemical assays

HCCLM3 cells were subjected to ultrasonic lysis and subsequent centrifugation. The supernatant was retained for metabolic assays. Following the protocols provided with the glucose (BC2505, Solarbio, Beijing, China), lactate (BC2235, Solarbio), and ATP (BC0305, Solarbio) assay kits, working solutions were incubated and absorbance measurements were taken at 505 nm, 570 nm, and 340 nm respectively using a microplate reader.

Glycolytic capacity was measured via ECAR using a Seahorse XFe24 Analyzer. Cells were plated, adhered, and incubated in CO_2-free medium for 1 h. ECAR was quantified after sequential injection of 10 mM glucose (50-99-7, Sigma, St. Louis, MO, USA), 2 mM oligomycin (495455, Sigma), and 50 mM 2-DG (D8375, Sigma) using standardized measurement cycles (3 min mix, 2 min wait, 3 min measure). After completing the ECAR kinetic measurements, a parallel CCK-8 assay was immediately performed on the same wells to obtain OD450 values as an indicator of the final number of viable cells. The raw ECAR (mpH/min) data from the Seahorse software were background-corrected and then normalized to the corresponding CCK-8 OD450 values. Finally, all ECAR data were presented as mpH/min/10^5 cells.

Wound healing assay

We assessed HCC cell migration using a wound healing assay. Cells were cultured in 6-well plates until they reached 90% confluence. A sterile pipette tip was used to create a linear scratch in the monolayer. After washing with PBS to remove debris, serum-free medium was added. Images were taken at 0 h and 24 h under a microscope, and wound closure was quantified with ImageJ software to calculate the healing rate.

Cell invasion and migration assays

Cell migration and invasion were assessed using Transwell chambers (8 μm pore size, Corning). For invasion assays, membranes were pre-coated with Matrigel (C0372, Beyotime, Shanghai, China). HCC cells (5×10^4 cells/well) were seeded in the upper chamber, while the lower chamber contained medium with 10% FBS as a chemoattractant. After 24 h incubation at 37 °C and 5% CO_2, non-migrated/invaded cells were removed from the upper membrane surface with a cotton swab. Membranes were fixed with methanol for 15 min and stained with 0.1% crystal violet (V5265, Sigma) for 15 min. Cells in five random fields per membrane were imaged and counted microscopically.

Dual-luciferase assay

Bioinformatic prediction of miR-500a-3p binding sites within the SOCS2 3'-UTR was performed using TargetScan Release 8.0. The SOCS2 3'-UTR wild-type (WT) and mutant (MUT) luciferase reporter constructs, based on the pmirGLO backbone, were synthesized and provided by GenePharma (the

3'-UTR sequences are shown in Fig. 3C). These plasmids were co-transfected into cells with miR-500a-3p mimics or negative control (mimics-NC) via Lipofectamine 2000. Luciferase activity was quantified 48 h post-transfection using the Dual-Luciferase Reporter Assay System (E1910, Promega, Madison, Wisconsin, USA). Working solutions were prepared according to the manufacturer's instructions. After removing the old medium, PLB lysis buffer was added at 100 µl/well and lysed on a horizontal shaker for 25 min. The lysate was collected into EP tubes for subsequent use. In clean EP tubes, 50 µl of LAR II working solution and 10 µl of lysate were added for firefly luciferase detection using a multifunctional microplate reader, followed by the addition of Stop & Glo Reagent (50 µl) for Renilla luciferase detection. Data were statistically analyzed using GraphPad Prism 9.

Flow cytometry

Apoptosis was evaluated by staining cells with the Annexin V-FITC/PI apoptosis detection kit (HY-K1073, MCE) according to the manufacturer's instructions. Quantification of apoptotic cells was performed using a BD Biosciences flow cytometer (Franklin Lake, NJ, USA).

Xenograft mouse model

A xenograft tumor model was established to assess the role of miR-500a-3p *in vivo*. 27 male BALB/C nude mice (6–8 weeks old), sourced from the Experimental Animal Center of Wuhan University, were maintained under SPF conditions with free access to food and water. MHCC97 cells transfected with mimics-miR-500a-3p or mimics-NC were trypsinized and resuspended at 2×10^7 cells/ml. Mice were randomized into three groups (n = 9): Control, mimics-NC, and mimics-miR-500a-3p. Each mouse was administered bilateral subcutaneous injections of 0.1 ml cell suspension into the axillae. General health, diet, and activity were monitored throughout the study. Starting from day 7 of the experiment, tumor volumes were measured weekly using a digital caliper. Length (L) was defined as the longest dimension of the tumor, and width (W) as the longest dimension perpendicular to the length. Tumor volume was calculated using the formula: volume = $(L \times W^2)/2$. At the end of week 4, mice were euthanized by cervical dislocation, and tumor tissues were immediately excised on ice and weighed. A portion of each tumor was fixed in 4% PFA for histological examination. For RNA-related analyses, fresh tumor tissue was immediately immersed in RNA stabilization solution (AM7024, Invitrogen), incubated at 4 °C overnight, and then transferred to –80 °C for long-term storage. Ethical approval was granted by Xiantao First People's Hospital, Affiliated Hospital of Hubei University of Science and Technology (approval number: 2024-01-018).

Immunohistochemistry

Tumor tissues from mice were processed by fixation in 4% PFA (24 h), dehydration, paraffin embedding, and sectioning at 4 µm. Deparaffinized and rehydrated sections were washed with PBS. To quench endogenous peroxidase, 100 µl of 3% H_2O_2 was applied for 10 min. Antigen retrieval was conducted in boiling buffer (E673002, Sangon) for 15 min. Non-specific binding was blocked with 5% BSA (20 min), and sections were probed with primary antibodies targeting Ki67 (1:1000, 28074-1-AP, Proteintech) and SOCS2 (1:200, bs-1896R, Bioss) overnight at 4 °C. After PBS washes, sections were incubated with secondary antibody (1:10000, 31460, Invitrogen) for 50 min. DAB (P0202, Beyotime) was used for visualization, and hematoxylin was employed for nuclear counterstaining. Imaging was performed using a microscope (Primo star, Carl Zeiss AG).

TUNEL staining

Dewaxed and rehydrated tumor tissue sections were subjected to TUNEL assay (T2130, Solarbio) according to the manufacturer's protocol. Briefly, the TUNEL reaction solution was added and incubated at 37 °C for 1 h. Nuclear counterstaining was carried out using DAPI (ab285390, Abcam). TUNEL-positive cells were visualized and quantified under a fluorescence microscope (LSM 910, Zeiss, Oberkochen, Germany) to determine apoptotic activity.

Western blot

Cellular or tissue proteins were extracted by ice-cold lysis in RIPA buffer (R0010, Solabio) for 20 min. Protein concentrations were determined with the BCA protein quantification kit. After separation by SDS-PAGE, proteins were transferred to PVDF membranes (88520/88518, Invitrogen) and blocked (5% BSA; ANT101L, AntGene, Wuhan, China) for 1 h. Membranes were washed with TBST and probed overnight at 4 °C with specific primary antibodies: p-STAT3 (1:500, PSTAT3-340AP, Invitrogen), STAT3 (1:2000, MA5-35302, Invitrogen), Bax (1:1000, MA5-16322, Invitrogen), Bcl-2 (1:1000, PA5-27094, Invitrogen), β-actin (1:1000, MA5-33078, Invitrogen), SOCS2 (1:1000, PA5-17219, Invitrogen), Cleaved-caspase3 (1:500, ab32042, Abcam), caspase3 (1:5000, ab32351, Abcam), p-STAT5 (1:500, PA5-104920, Invitrogen), STAT5 (1:1000, 71-2500, Invitrogen), p-JAK2 (1:1000, MA5-42424, Invitrogen), and JAK2 (1:1000, 702434, Invitrogen). After washing, membranes were incubated with goat anti-rabbit secondary antibody (1:10000, 31460, Invitrogen) for 2 h. Detection was carried out using the Super ECL detection kit (E-IR-R307, Elabscience), and bands were quantified with ImageJ software.

Statistical analyses

Data are expressed as mean ± SD. The Shapiro–Wilk test was used to assess the distribution of all datasets, and the results indicated that all data conformed to the criteria for normal distribution. Student's t-test was used for comparisons between two groups, while one-way ANOVA followed by Tukey's *post-hoc* test was applied for analyses involving multiple groups. A P-value < 0.05 was considered statistically significant. Graphs were plotted with GraphPad Prism 9.0.

Results

Upregulation of miR-500a-3p expression in HCC cells

Analysis of miR-500a-3p expression via qRT-PCR showed a significant increase in HCC patient tissues relative to matched normal adjacent tissues (Fig. 1A). Analysis based on the TCGA-LIHC database showed that the expression of miR-500a-3p was significantly higher in primary liver cancer tissues compared to normal tissues (Fig. 1B). *In vitro* comparisons revealed that miR-500a-3p was markedly overexpressed in HCC cell lines compared to THLE-2 normal hepatocytes, with HCCLM3 cells showing the most pronounced upregulation (Fig. 1C). Furthermore, Kaplan–Meier survival analysis using the GEPIA database demonstrated that patients with high miR-500a-3p expression had significantly lower overall survival rates compared to those with low expression (Fig. 1D). In summary, miR-500a-3p is upregulated in HCC cells and is associated with reduced patient survival, suggesting its potential as a diagnostic biomarker and therapeutic target for HCC.

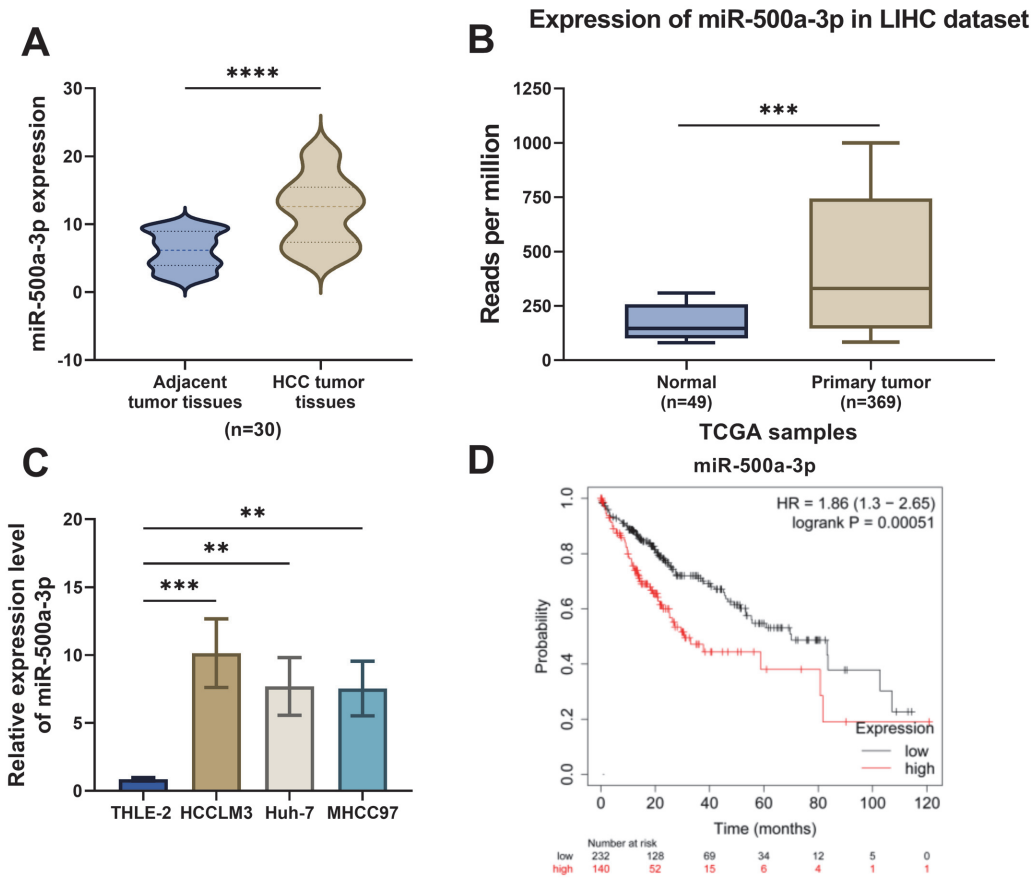

Fig. 1. Upregulation of miR-500a-3p in HCC cells. (**A**) miR-500a-3p levels in HCC and adjacent normal tissues via qRT-PCR. (**B**) TCGA-LIHC data showing miR-500a-3p in normal (n = 49) and HCC (n = 369) tissues. (**C**) qRT-PCR detection of miR-500a-3p levels in normal human hepatocytes and HCC cells. Data are presented as the mean ± SD from six independent experiments. (**D**) Survival analysis of HCC patients with high or low miR-500a-3p expression. ** P < 0.01, *** P < 0.001, **** P < 0.0001.

miR-500a-3p promotes proliferation and glycolysis, and inhibits apoptosis in HCC cells

qRT-PCR analysis confirmed successful transfection, with miR-500a-3p expression significantly upregulated in the mimics-miR-500a-3p group compared to mimics-NC, and downregulated in the anti-miR-500a-3p group relative to anti-NC (Fig. 2A). Colony formation assays revealed that miR-500a-3p overexpression enhanced HCCLM3 cell proliferation, while its inhibition suppressed it (Fig. 2B–C). Wound healing assays indicated that miR-500a-3p overexpression promoted cell migration (Fig. 2D–E), and Transwell assays further demonstrated its role in enhancing invasion and migration (Fig. 2F–H). Conversely, miR-500a-3p inhibition attenuated these malignant phenotypes.

During glycolysis, high glucose consumption and lactate production indicate active glycolytic pathways, and glycolysis-derived ATP reflects the energy supply capacity of this pathway (Tufail et al., 2024). As lactate production and release acidify the extracellular environment, ECAR is commonly used as an indirect indicator of glycolytic activity (Zhu et al., 2025). Overexpression of miR-500a-3p markedly enhanced glycolytic metabolism, as evidenced by increased glucose consumption, lactate production (Fig. 2I–J), elevated ECAR (Fig. 2K–L), and higher ATP levels (Fig. 2M). Conversely, miR-500a-3p inhibition suppressed glycolysis. Flow cytometry analysis showed that miR-500a-3p overexpression reduced apoptosis, while its inhibition promoted cell death (Fig. 2N–O). Western blot results further demonstrated that miR-500a-3p overexpression downregulated Bax and Cleaved-caspase3/caspase3 ratio while upregulating Bcl-2 (Fig. 2P–Q). Inhibition of miR-500a-3p reversed these effects. Collectively, miR-500a-3p drives HCC malignancy by enhancing proliferation, migration, invasion, glycolysis, and suppressing apoptosis.

miR-500a-3p targets and regulates SOCS2

In this study, multiple bioinformatics databases including miRWalk, TargetScanHuman 8.0, miRDB, and UALCAN were utilized for screening, identifying SOCS2 as a potential target gene of miR-500a-3p (Fig. 3A). Expression analysis based on the TCGA-LIHC database revealed that SOCS2 expression was significantly lower in primary liver cancer tissues compared to normal liver tissues (Fig. 3B). TargetScanHuman 8.0 predicted the potential binding sites between miR-500a-3p and SOCS2 (Fig. 3C), which were subsequently validated by dual-luciferase reporter assays. The results demonstrated that overexpression of miR-500a-3p significantly suppressed luciferase activity of SOCS2-3'UTR-WT, whereas the effect on SOCS2-3'UTR-MUT was negligible (Fig. 3D). Additionally, qRT-PCR analysis showed that SOCS2 expression in HCC patient tissues was markedly lower than in adjacent normal tissues (Fig. 3E). Kaplan–Meier survival analysis using the GEPIA database indicated that low SOCS2 expression correlates with poorer survival in HCC patients (Fig. 3F). Western blot analysis further demonstrated inverse regulation, with miR-500a-3p overexpression suppressing and inhibition enhancing SOCS2 protein levels (Fig. 3G–H), confirming SOCS2 as a direct target of miR-500a-3p.

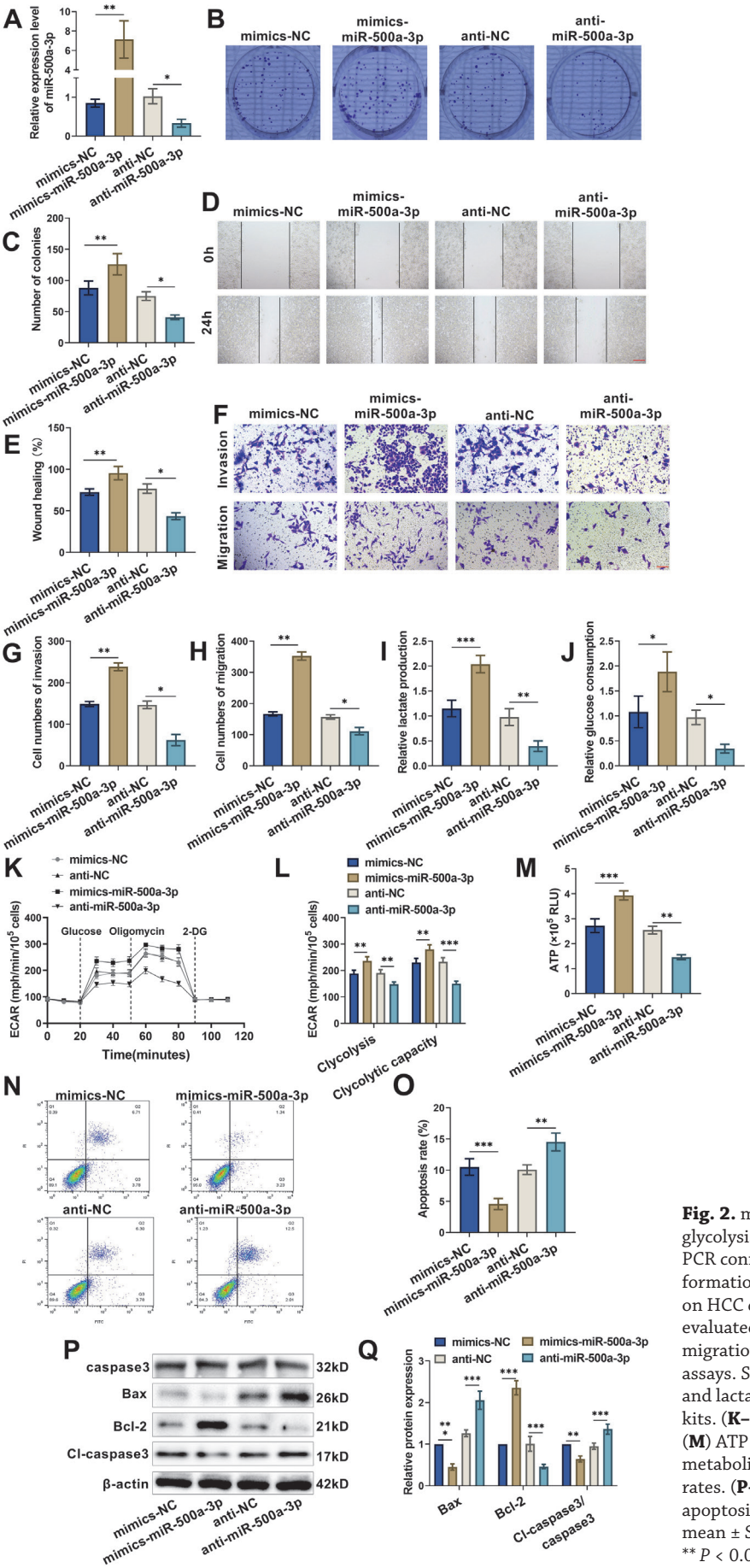

Fig. 2. miR-500a-3p promotes proliferation and glycolysis, and inhibits apoptosis in HCC cells. (**A**) qRT-PCR confirmed transfection efficiency. (**B–C**) Colony formation assays determined the impact of miR-500a-3p on HCC cell proliferation. (**D–E**) Wound healing assays evaluated migratory ability. Scale bar: 200 μm. (**F–H**) Cell migration and invasion were examined using Transwell assays. Scale bar: 100 μm. (**I–J**) Glucose consumption and lactate production were quantified with assay kits. (**K–L**) ECAR analysis assessed glycolytic capacity. (**M**) ATP content was measured to evaluate energy metabolism. (**N–O**) Flow cytometry detected apoptosis rates. (**P–Q**) Western blotting measured expression of apoptosis-related proteins. Data are presented as the mean ± SD from six independent experiments. * $P < 0.05$, ** $P < 0.01$, *** $P < 0.001$.

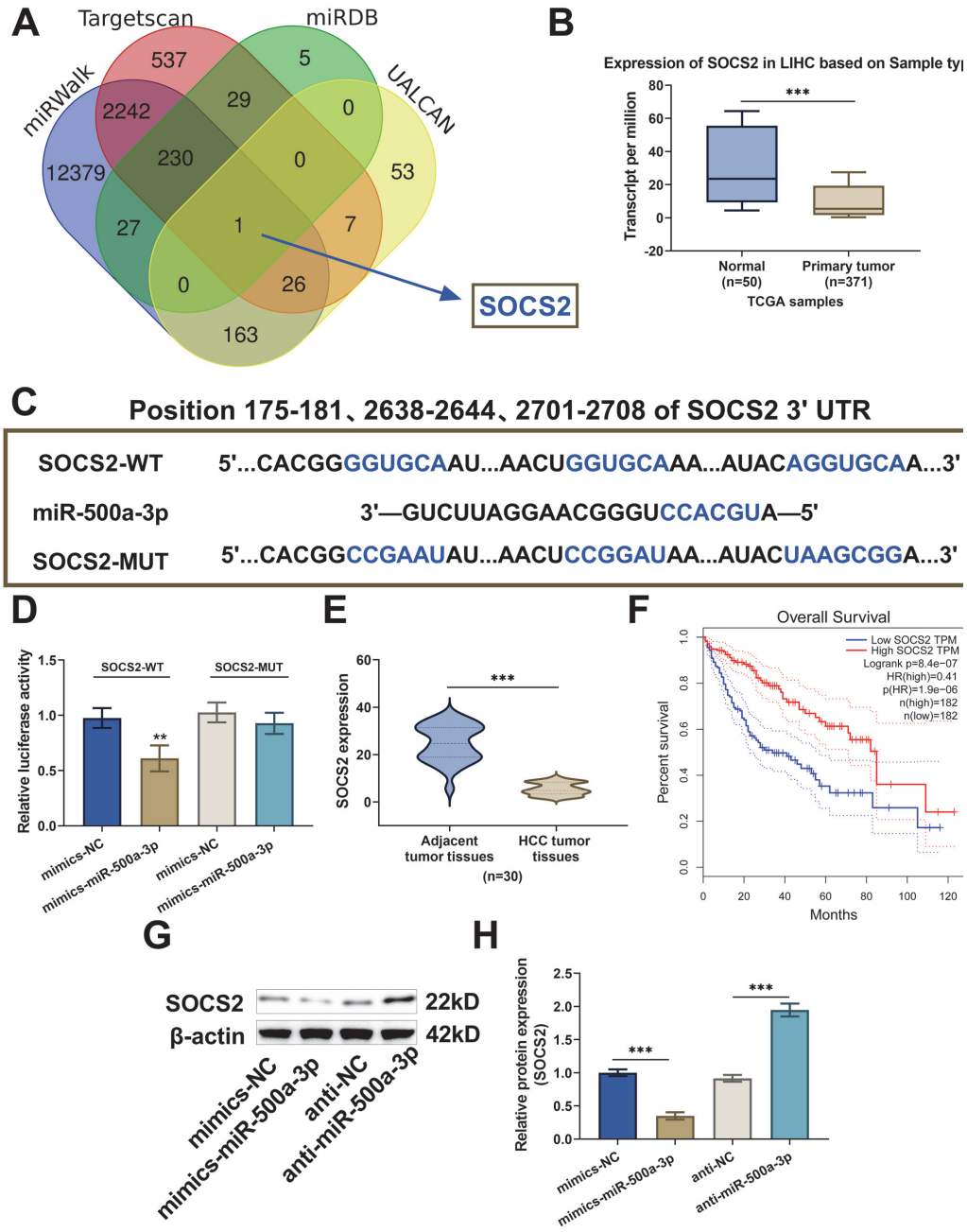

Fig. 3. miR-500a-3p targets and regulates SOCS2. (**A**) Venn diagram of bioinformatics databases showing overlapping miR-500a-3p target genes. (**B**) SOCS2 expression in normal and HCC tissues from TCGA-LIHC. (**C**) TargetScan Release 8.0 predicted SOCS2 3'-UTR binding sites for miR-500a-3p. (**D**) Dual-luciferase assay testing miR-500a-3p's effect on SOCS2. Data are presented as the mean ± SD from six independent experiments. (**E**) SOCS2 expression in HCC tissues and paired adjacent normal tissues from 30 patients was assessed using qRT-PCR. (**F**) Survival analysis of HCC patients with high or low SOCS2 expression. (**G–H**) Western blot of SOCS2 protein levels after miR-500a-3p modulation. ** $P < 0.01$, *** $P < 0.001$.

Overexpression of SOCS2 reverses the regulatory effects of miR-500a-3p on proliferation, glycolysis, and apoptosis in HCC cells

The successful transfection and overexpression of SOCS2 were confirmed via Western blot analysis (Fig. 4A–B). A significant reduction in SOCS2 protein was observed in the mimics-miR-500a-3p+Vector group relative to the mimics-NC+Vector group, which corroborates that miR-500a-3p directly targets and inhibits SOCS2. Subsequent SOCS2 overexpression counteracted this miR-500a-3p-mediated suppression (Fig. 4C–D). Functional assays revealed that miR-500a-3p overexpression enhanced colony formation, migration, and invasion (Fig. 4E–K). These oncogenic phenotypes were partially rescued by SOCS2 upregulation. Moreover, miR-500a-3p mimicry promoted glycolytic metabolism, as evidenced by elevated glucose consumption (Fig. 4L), lactate production (Fig. 4M), ECAR (Fig. 4N–O), and ATP levels (Fig. 4P). All these metabolic effects were markedly attenuated by SOCS2 overexpression. At the molecular level, miR-500a-3p decreased the expression of the pro-apoptotic protein Bax and the Cleaved-caspase3/

caspase3 ratio, but increased the anti-apoptotic protein Bcl-2 (Fig. 4Q–R). These alterations in apoptosis-related proteins were likewise reversed by SOCS2. Collectively, these findings demonstrate that SOCS2 acts as a key downstream mediator of miR-500a-3p, able to reverse its effects on cellular proliferation, motility, glycolytic reprogramming, and apoptosis.

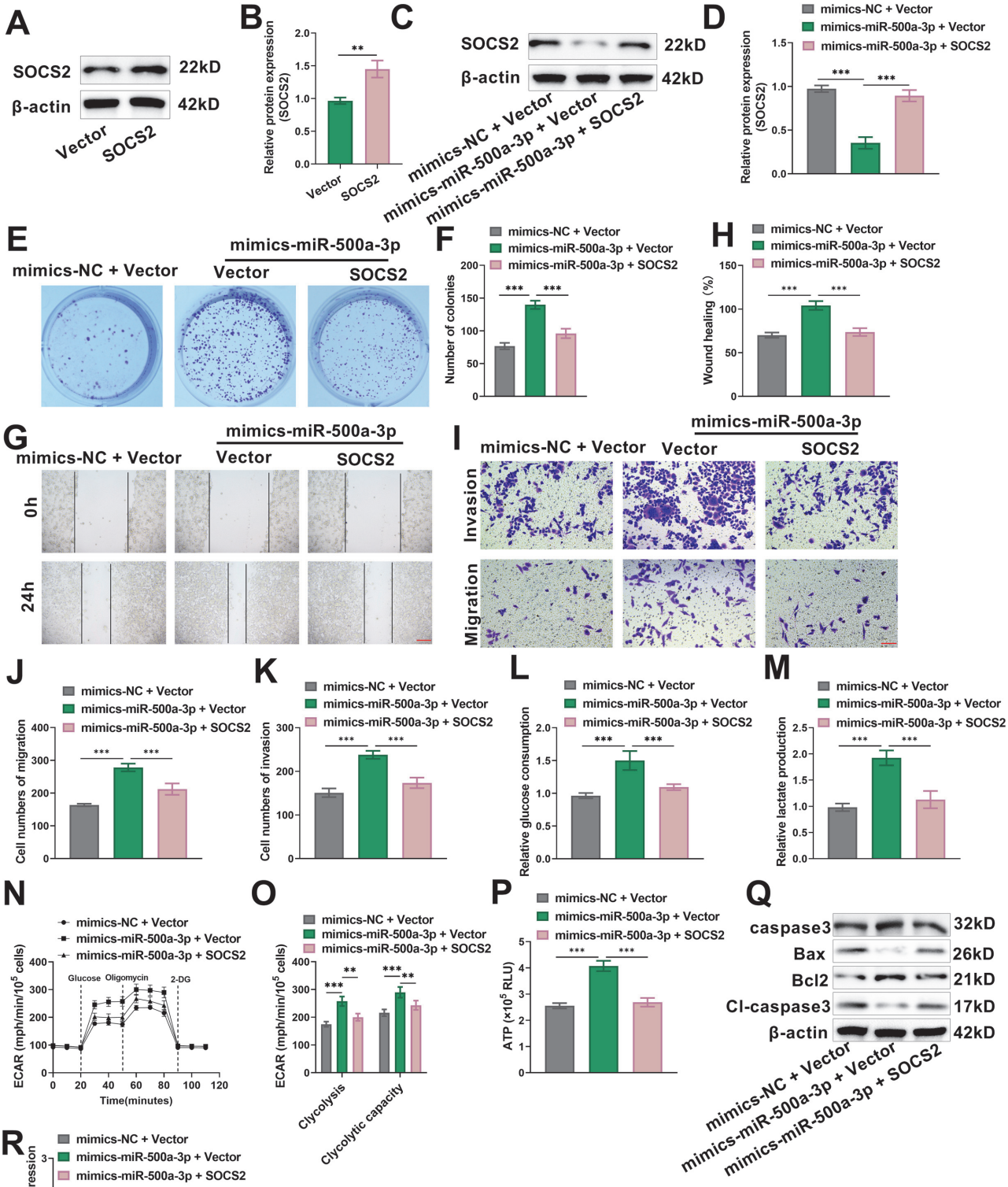

Fig. 4. Overexpression of SOCS2 reverses the regulatory effects of miR-500a-3p on proliferation, glycolysis, and apoptosis in HCC cells. (**A–B**) Western blot for SOCS2 overexpression efficiency. (**C–D**) SOCS2 protein levels and miR-500a-3p regulation. (**E–F**) Colony formation assay for proliferation. (**G–H**) Wound healing assay for migration. Scale bar: 200 μm. (**I–K**) Transwell assay for migration/invasion. Scale bar: 100 μm. (**L–M**) Glucose uptake and lactate secretion measured by kits. (**N–O**) ECAR analysis of glycolysis. (**P**) ATP content quantified. (**Q–R**) Western blot for apoptotic proteins (Bax, Bcl-2, Cleaved-caspase3, caspase3). Data are presented as the mean ± SD from six independent experiments. ** $P < 0.01$, *** $P < 0.001$.

miR-500a-3p regulates the proliferation, glycolysis, and apoptosis of HCC cells via the JAK2/STAT5 pathway by suppressing SOCS2

Aberrant activation of the JAK2/STAT5 pathway is strongly linked to HCC pathogenesis (Cong et al., 2020; Guvenir Celik and Eroglu, 2023; Shires et al., 2023). Western blot analysis showed that, compared with the mimics-NC group, overexpression of miR-500a-3p significantly increased the phosphorylation levels of p-JAK2/JAK2, p-STAT5/STAT5, and p-STAT3/STAT3 in HCCLM3 and MHCC97 cells (Fig. 5A–D). In contrast, inhibition of miR-500a-3p reduced the phosphorylation levels of these proteins. To further validate the regulatory effect of miR-500a-3p on the JAK2/STAT5 pathway, the JAK2 inhibitor Fedratinib (0.2 μM) and the JAK2/STAT5 agonist EPO (200 U/ml) were used for intervention (Suppl. Fig. S1). In HCCLM3 cells, compared with the miR-500a-3p group, the mimics-miR-500a-3p+SOCS2 group exhibited markedly decreased phosphorylation levels of JAK2 and STAT5, markedly increased SOCS2 protein expression, and no obvious change in STAT3 phosphorylation (Fig. 5E–F). Fedratinib treatment also reversed miR-500a-3p-induced JAK2/STAT5 activation and further suppressed STAT3 phosphorylation, but had no significant effect on SOCS2 expression. Compared with the mimics-miR-500a-3p+SOCS2 group, additional EPO treatment enhanced JAK2/STAT5 pathway activity, while exerting no significant effect on SOCS2 expression or STAT3 phosphorylation. In MHCC97 cells, SOCS2 overexpression similarly reduced the phosphorylation levels of JAK2 and STAT5, increased SOCS2 protein expression, and did not affect STAT3 phosphorylation (Fig. 5G–H). Fedratinib treatment produced effects similar to those of SOCS2 overexpression. Compared with the mimics-miR-500a-3p+SOCS2 group, additional EPO treatment not only enhanced JAK2/STAT5 signaling activity, but also led to a marked decrease in SOCS2 protein expression, while still showing no obvious impact on STAT3 phosphorylation. These findings indicate that miR-500a-3p promotes the phosphorylation of JAK2 and STAT5 and thereby activates the JAK2/STAT5 signaling pathway by regulating SOCS2 expression, whereas SOCS2 upregulation or pharmacological intervention can suppress the activity of this pathway, suggesting that miR-500a-3p plays an important role in the regulation of JAK2/STAT5 signaling.

Cellular experiments showed that SOCS2 overexpression or Fedratinib treatment reversed the miR-500a-3p-induced enhancement of colony formation (Fig. 5I–J), as well as cell migration and invasion (Fig. 5K–O). In addition, SOCS2 overexpression or Fedratinib treatment reduced miR-500a-3p-induced glucose consumption (Fig. 5P), ATP production (Fig. 5Q), lactate generation (Fig. 5R), glycolysis, and glycolytic capacity (Fig. 5S–T). Western blot analysis further revealed that SOCS2 overexpression or Fedratinib treatment reversed the regulatory effects of miR-500a-3p on apoptosis-related proteins, thereby promoting cell apoptosis (Fig. 5U–V). Notably, compared with the mimics miR-500a-3p+SOCS2 group, combined treatment with EPO reversed these changes. These results demonstrate that SOCS2 overexpression or Fedratinib treatment can effectively counteract the pro-tumorigenic effects mediated by miR-500a-3p, whereas combined EPO treatment can further reverse the SOCS2-mediated regulation of these cellular behaviors.

To further verify the function of STAT5, stable si-STAT5 and oe-STAT5 cell lines were generated in HCCLM3 and MHCC97 cells. Western blot analysis confirmed that si-STAT5 effectively reduced STAT5 and its phosphorylation, while oe-STAT5 significantly increased the levels of STAT5 and p-STAT5 (Fig. 6A–E). Silencing STAT5 markedly suppressed the viability of HCC cells, whereas STAT5 overexpression significantly enhanced HCC cell viability (Fig. 6F–I). Functional assays demonstrated that STAT5 knockdown notably inhibited the migratory capacity (Fig. 6J–L) and invasive capacity (Fig. 6M–O) of HCC cells, reduced glucose uptake (Fig. 6P–Q), lactate production (Fig. 6R–S), and ATP levels (Fig. 6T–U), while simultaneously promoting cell apoptosis (Fig. 6V–Y). In contrast, STAT5 overexpression produced opposite effects. These findings demonstrate that STAT5 plays a key promotive role in the proliferation, migration, invasion, and energy metabolism of HCC cells, serving as a critical downstream effector of the miR-500a-3p/SOCS2 axis in the regulation of the JAK2/STAT5 signaling pathway and tumor progression.

miR-500a-3p promotes tumor growth in tumor-bearing mice

This study validated the pro-tumorigenic role of miR-500a-3p *in vivo* using animal experiments. The results demonstrated a significant increase in tumor volume and final weight in the miR-500a-3p overexpression group relative to controls (Fig. 7A–C). Immunohistochemical analysis showed that the expression level of the proliferation marker Ki67 was significantly increased in tumor tissues from the miR-500a-3p overexpression group (Fig. 7D–E), and H&E staining revealed more pronounced malignant pathological features (including anisokaryosis and hemorrhage). TUNEL assays demonstrated that the apoptosis rate of tumor cells was markedly reduced in the miR-500a-3p overexpression group (Fig. 7F–G). Immunohistochemistry further indicated that SOCS2 protein expression was significantly downregulated in tumor tissues from the miR-500a-3p overexpression group (Fig. 7H–I). Western blot analysis confirmed that miR-500a-3p overexpression decreased SOCS2 expression while increasing the phosphorylation levels of p-JAK2/JAK2 and p-STAT5/STAT5 (Fig. 7J–K). qPCR results showed that the level of miR-500a-3p in tumor tissues of mice in the miR-500a-3p overexpression group was significantly higher than that in the NC group (Fig. 7L). Collectively, these *in vivo* findings indicate that miR-500a-3p drives tumor growth by promoting proliferation and suppressing apoptosis, mediated through SOCS2 inhibition and subsequent activation of the JAK2/STAT5 axis.

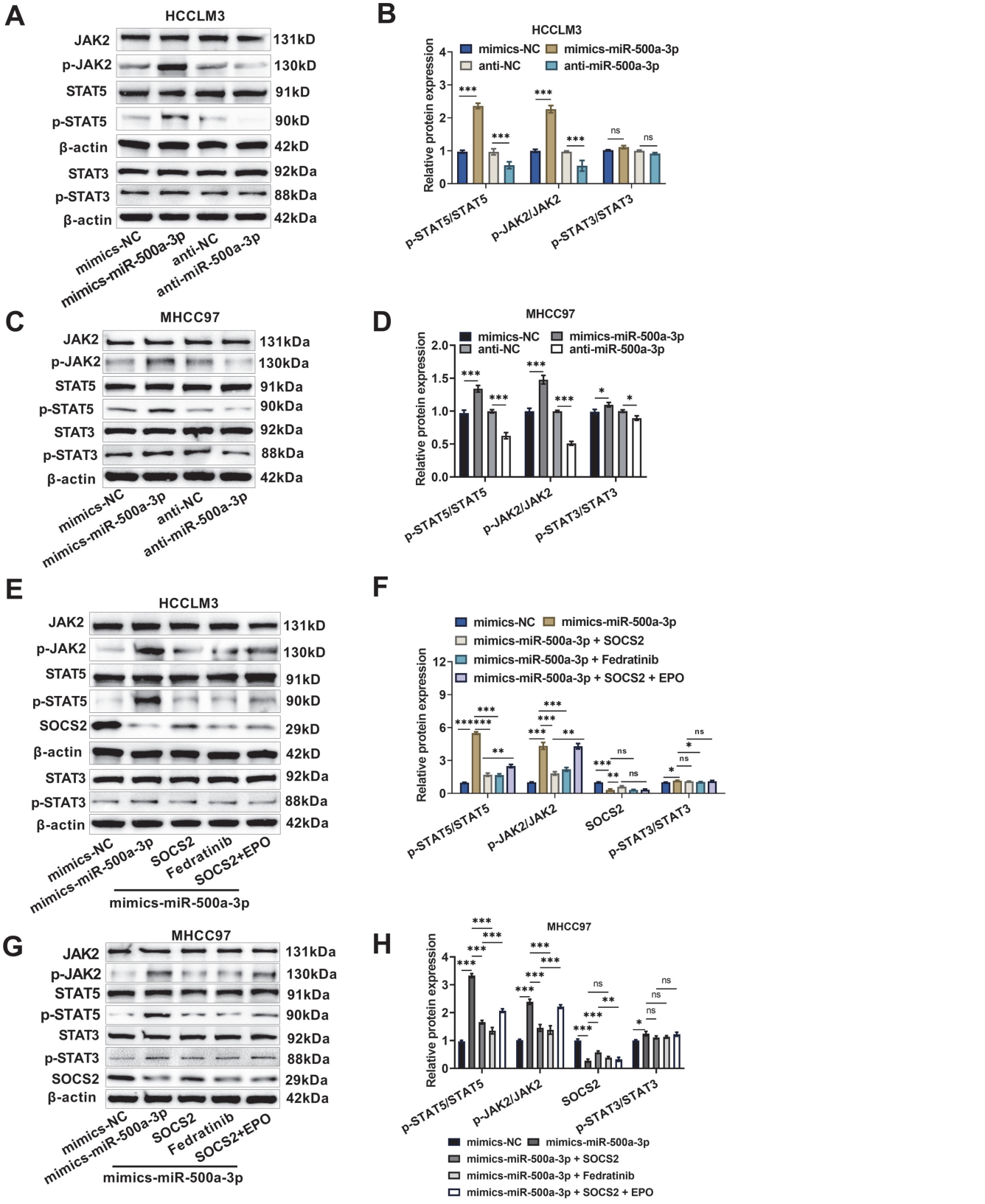

Fig. 5. miR-500a-3p regulates the proliferation, glycolysis, and apoptosis of HCC cells via the JAK2/STAT5 pathway by suppressing SOCS2. (**A–D**) Western blot analysis of the phosphorylation levels of p-JAK2/JAK2, p-STAT5/STAT5, and p-STAT3/STAT3 in HCCLM3 and MHCC97 cells. (**E–H**) Western blot analysis examining the effects of SOCS2 overexpression or drug treatment (Fedratinib/EPO) on the phosphorylation of JAK2, STAT5, and STAT3 in HCCLM3 and MHCC97 cells (*continued on the next page*).

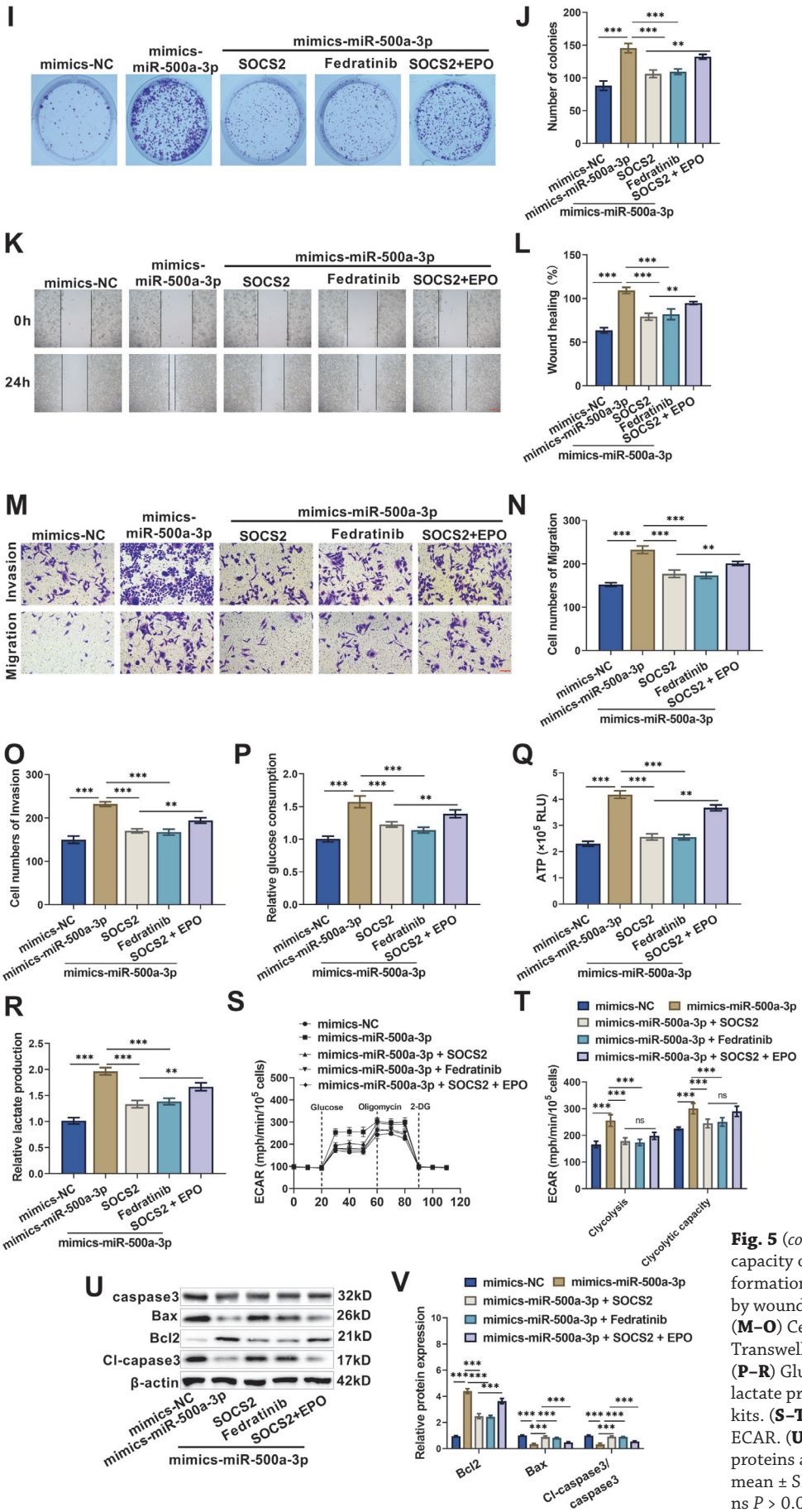

Fig. 5 (*continued*). (**I–J**) The proliferative capacity of cells was assessed by colony formation assay. (**K–L**) Cell migration assessed by wound healing assay. Scale bar: 200 μm. (**M–O**) Cell migration and invasion analyzed by Transwell assay. Scale bar: 100 μm. (**P–R**) Glucose consumption, ATP content, and lactate production quantified using commercial kits. (**S–T**) Glycolytic capacity measured by ECAR. (**U–V**) Expression of apoptosis-related proteins analyzed. Data are presented as the mean ± SD from six independent experiments. ns $P > 0.05$, * $P < 0.05$, ** $P < 0.01$, *** $P < 0.001$.

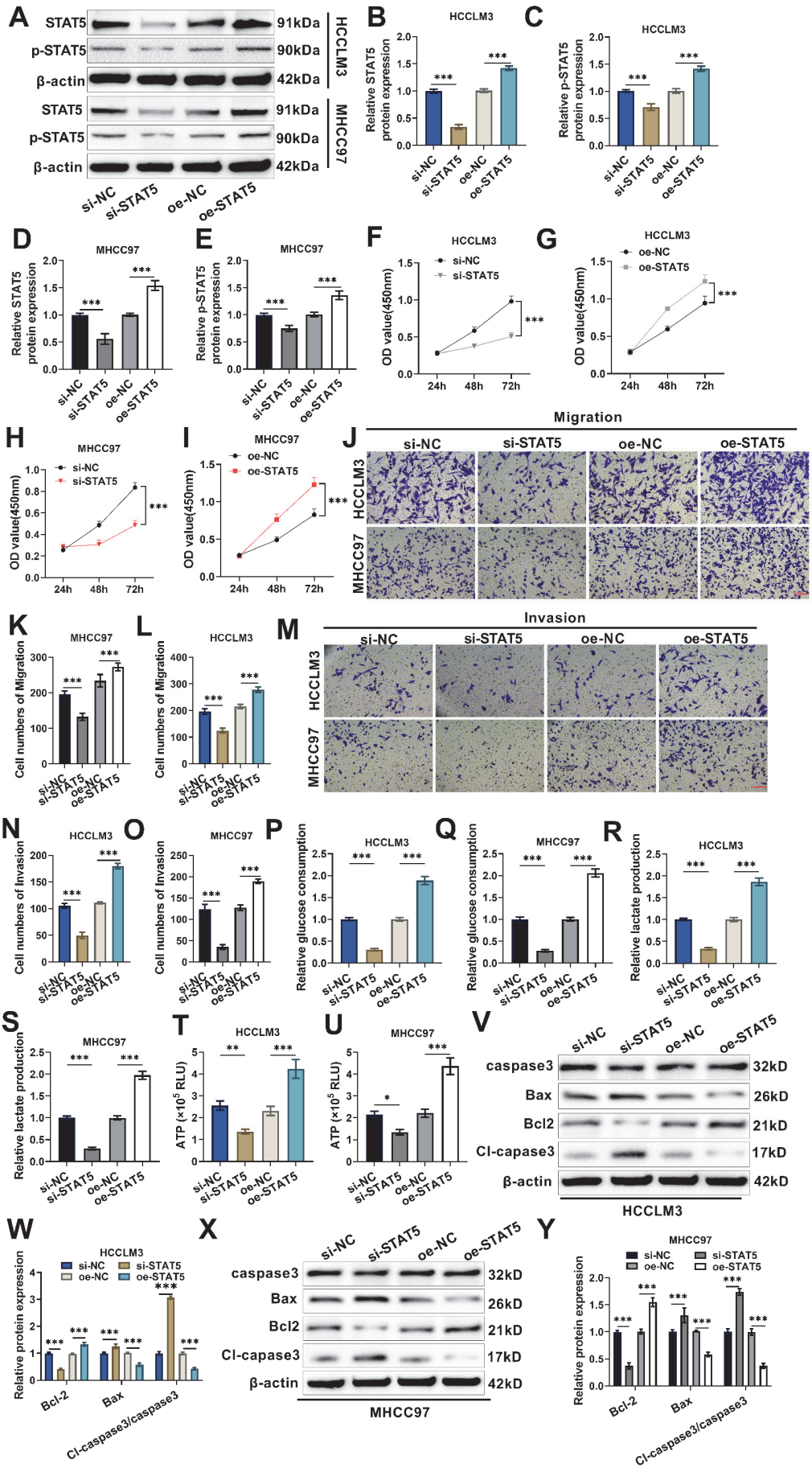

Fig. 6. STAT5 promotes proliferation and glycolysis while suppressing apoptosis in HCC cells and serves as a key downstream effector of the miR-500a-3p/SOCS2 axis. (**A–E**) Western blot analysis of the construction efficiency of si-STAT5 and oe-STAT5. (**F–O**) Cell viability, migration, and invasion assays evaluating the effects of STAT5 silencing or overexpression on hepatocellular carcinoma cell behavior. (**P–U**) Assessment of the regulatory effects of STAT5 silencing or overexpression on cellular glucose uptake, lactate production, and ATP levels. (**V–Y**) Detection of apoptosis-related proteins (Bax, Bcl-2, Cleaved-caspase3, caspase3) following STAT5 silencing or overexpression. Data are presented as mean ± SD from six independent experiments. ** $P < 0.01$, *** $P < 0.001$.

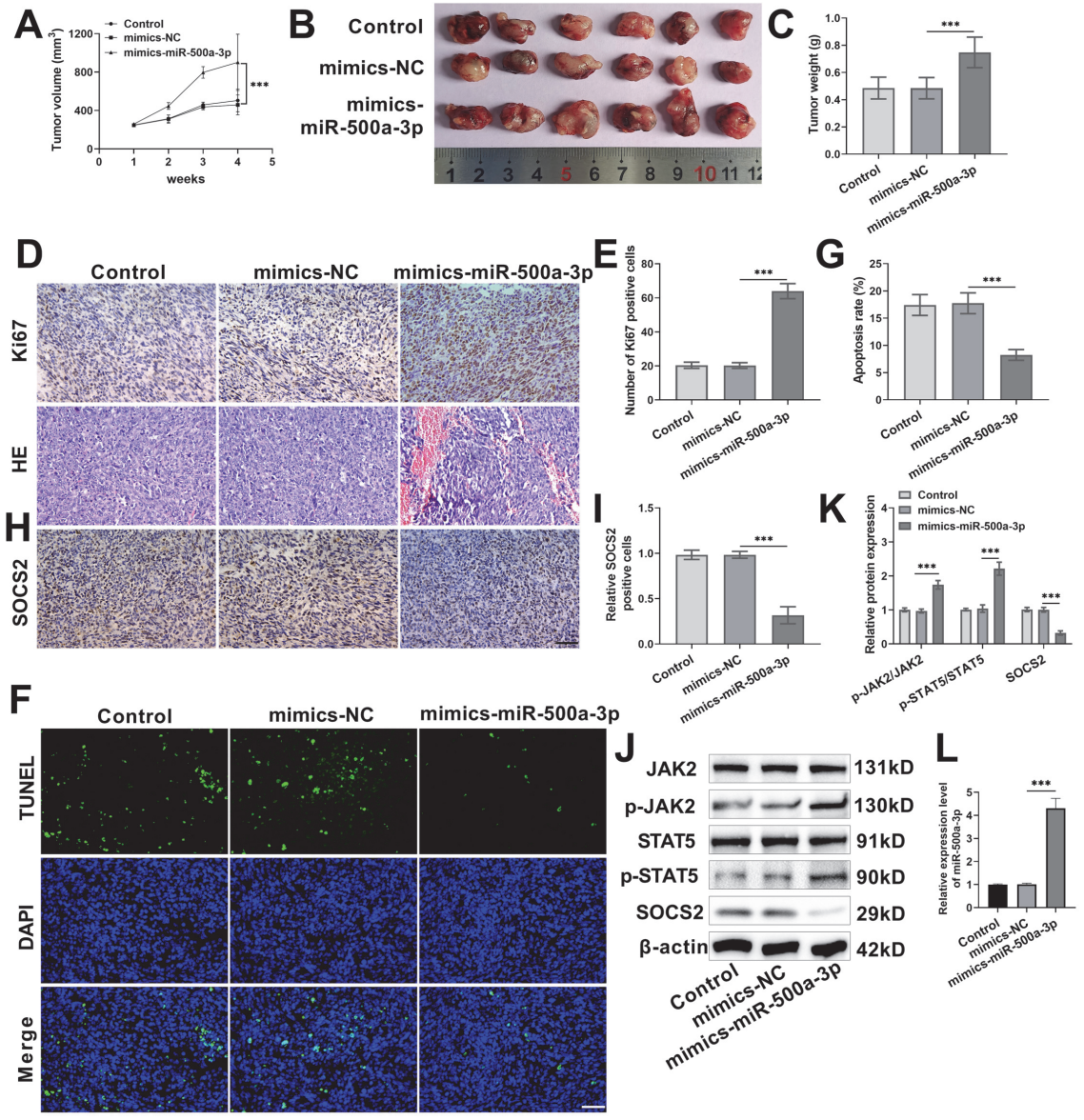

Fig. 7. miR-500a-3p promotes tumor growth in tumor-bearing mice. (**A**) Tumor volume growth curve over 4 weeks. (**B**) From each group, six tumors were selected for imaging to observe the gross morphology of the tumor tissues in mice. (**C**) Final tumor weight at day 28. (**D–E**) IHC analysis of Ki67 expression and HE staining showing histopathological features. Scale bar: 50 μm. (**F–G**) Apoptosis assessed by TUNEL assay. Scale bar: 50 μm. (**H–I**) SOCS2 protein expression detected by IHC. (**J–K**) Western blot analysis of SOCS2 and JAK2/STAT5 pathway proteins. (**L**) qPCR analysis of miR-500a-3p expression levels at the experimental endpoint. Data are presented as mean ± SD from nine biological replicates. *** $P < 0.001$.

Discussion

miRNAs play dual roles in cancer development and progression, functioning as both oncogenes and tumor suppressors (Shen et al., 2022). In HCC research, miRNAs such as miR-21, miR-155, miR-223, and miR-375 have been systematically investigated and have shown significant value in the diagnosis, prognostic prediction, and therapeutic response assessment of HCC, making them relatively "mature" molecular markers (Aziz et al., 2022; Eldosoky et al., 2023; Li et al., 2021). In recent years, the oncogenic function and clinical significance of miR-500a-3p have attracted increasing attention, and it has been considered a novel miRNA worthy of further exploration in HCC (Long et al., 2022). This study aims to further elucidate the functional roles and underlying mechanisms of miR-500a-3p in the development and progression of HCC, and to provide a theoretical basis for its potential as a biomarker and therapeutic target. A marked elevation of miR-500a-3p expression was identified in HCC clinical samples and cultured cells, and this high expression level was strongly linked to adverse clinical outcomes. This is bolstered by existing literature; notably, a prior study demonstrated that miR-500a-3p drives HCC advancement by facilitating the preservation of stem-like cancer cells (Jiang et al., 2017). Analysis of the TCGA database further validated elevated miR-500a-3p expression in primary liver cancer and its association with reduced patient survival. Our *in vitro* functional assays demonstrated that miR-500a-3p

overexpression enhanced HCC cell proliferation, migration, invasion, and glycolytic metabolism, but suppressed apoptosis. These pro-oncogenic effects were reversed upon miR-500a-3p inhibition. This aligns with its documented role in other malignancies; for instance, in colorectal cancer, miR-500a-3p also facilitates proliferation and migration (Liu et al., 2022). These data corroborate that miR-500a-3p acts as a potent oncogene in HCC. We postulate that this discovery has significant translational clinical value, as miR-500a-3p could serve as a diagnostic and prognostic biomarker. Its detection in clinical samples (e.g., serum or biopsies) may provide a basis for early HCC screening and refined risk stratification strategies (Khare et al., 2022; Long et al., 2022). In addition, the potential of miRNAs as therapeutic targets is receiving increasing attention. Inhibition strategies targeting oncogenic miRNAs, such as the use of antimiRs or antisense oligonucleotides, can effectively block their function and thereby suppress tumor growth (Reda El Sayed et al., 2021; Shademan et al., 2025). In the future, combining miR-500a-3p inhibitors with other conventional or novel anticancer agents may achieve synergistic effects and improve the therapeutic efficacy for HCC.

Acting as key suppressors of the JAK/STAT pathway, SOCS proteins mediate the ubiquitin-dependent degradation of JAKs or directly block STAT phosphorylation (Keewan and Matlawska-Wasowska, 2021; Yan et al., 2024). Among them, SOCS2 is recognized for exerting tumor-suppressive effects in multiple cancer types. Its reduced expression is frequently correlated with advanced disease and poorer clinical outcomes. For instance, SOCS2 overexpression has been shown to suppress growth and invasion in colorectal and lung cancer models (Cabrera-Galván et al., 2023; Wang et al., 2022). The findings of this investigation confirm SOCS2's role as a tumor suppressor in HCC. A correlation was observed between low SOCS2 expression and poorer patient prognosis. Furthermore, SOCS2 upregulation effectively reversed the malignant characteristics promoted by miR-500a-3p, indicating its potential as a therapeutic target for HCC intervention. Critically, the regulation of SOCS proteins by miRNAs represents a fundamental mechanism of oncogenic or tumor-suppressive action. Our study identified SOCS2 as a direct target of miR-500a-3p via 3'-UTR binding, thereby repressing its expression. This discovery adds a significant layer of complexity to the oncogenic miRNA-mRNA network. This regulatory paradigm is not unique; other miRNAs, such as miR-761 which accelerates HCC progression by targeting SOCS2 (Zhou et al., 2022), are also known to modulate the JAK/STAT pathway and tumorigenesis through SOCS family regulation (Pang et al., 2025; Rahbar Farzam et al., 2024). Consequently, elucidating these intricate miRNA-SOCS interactions is crucial for developing precise molecular therapies. Correcting abnormal SOCS2 expression via gene editing technologies (such as CRISPR/Cas9), or developing small molecule drugs that can block miRNA-SOCS2 interactions, may provide new therapeutic opportunities for HCC patients (Amjad et al., 2024; Juaid et al., 2021). SOCS2 was verified as a direct target gene of miR-500a-3p through initial bioinformatic screening and subsequent validation via dual-luciferase reporter assays. The experimental data demonstrated that miR-500a-3p post-transcriptionally suppresses SOCS2 expression. Furthermore, analysis of HCC tissues revealed significant SOCS2 downregulation, and lower SOCS2 levels were associated with poorer patient prognosis, reinforcing its recognized role as a tumor suppressor in HCC.

The JAK/STAT pathway is pivotal for numerous biological processes, such as cell proliferation, differentiation, apoptosis, and immune regulation. Its aberrant activation is frequently implicated in the pathogenesis and advancement of various cancers, including colorectal, cervical, and pancreatic cancer, as well as HCC (Ghasemian et al., 2023; Guo et al., 2022; Raymant et al., 2024; Valle-Mendiola et al., 2023). This study found that overexpression of miR-500a-3p significantly increased the phosphorylation levels of JAK2, STAT3, and STAT5, whereas upregulation of SOCS2 markedly reduced the ratios of p-JAK2/JAK2 and p-STAT5/STAT5, with no notable impact on p-STAT3/STAT3. These results suggest that the regulation of STAT3 by miR-500a-3p may not occur primarily through SOCS2. Instead, the activation of STAT3 may occur via a bypass pathway of the JAK2/STAT5 axis (Zhou et al., 2025), while the negative regulatory role of SOCS2 is mainly focused on the JAK2/STAT5 branch. This study further demonstrated that overexpression of miR-500a-3p significantly enhanced the phosphorylation of JAK2 and STAT5, indicating that miR-500a-3p can activate the JAK/STAT signaling pathway. Functional experiments showed that si-STAT5 markedly inhibited HCC cell proliferation, migration, invasion, and glycolysis while promoting apoptosis, a pattern highly consistent with the effects mediated by the miR-500a-3p/SOCS2 axis. Together, these findings demonstrate that STAT5 is the key downstream effector molecule through which the miR-500a-3p/SOCS2 axis regulates the malignant phenotype of HCC cells, thereby establishing the specificity of the JAK2/STAT5 axis in this study. This effect was negated by SOCS2 overexpression or Fedratinib treatment, and partially rescued by EPO, demonstrating that miR-500a-3p activates the pathway specifically through SOCS2 inhibition. The resulting constitutive JAK2/STAT5 signaling was sufficient to promote proliferation, glycolysis, and apoptosis evasion in HCC cells, a conclusion highly consistent with prior reports on this pathway's role in cancer. Consistent with previous reports that JAK2/STAT5 inhibition suppresses colorectal cancer progression (Liu et al., 2025) and that STAT5 activation can inhibit HCC through CDYL2 expression (Chen et al., 2022), our functional analyses demonstrated that SOCS2 overexpression or JAK2 pharmacological inhibition reversed miR-500a-3p-mediated oncogenic phenotypes, including enhanced proliferation, migration, invasion, glycolysis, and apoptosis resistance. These results not only clarify the mechanistic role of the miR-500a-3p/SOCS2/JAK2/STAT5 axis in HCC but also offer novel perspectives for therapeutic targeting. Currently, various JAK/STAT inhibitors are being evaluated in preclinical and clinical studies for HCC (Park et al., 2023), and the results of this study provide a theoretical basis for their rational application.

Tumorigenesis and progression are a complex, multi-step, and multi-factorial process, in which unlimited cell proliferation, metabolic reprogramming, and evasion of apoptosis are the most prominent features (Jiang et al., 2025; Ren, 2024; Zhang et al., 2024). Our study not only verified the regulatory relationship between miR-500a-3p and the JAK2/STAT5 pathway but also, for the first time, revealed the role of this pathway in modulating glycolysis, proliferation, and apoptosis of hepatocellular carcinoma cells from a metabolic perspective. Ectopic expression of miR-500a-3p significantly augmented the proliferative, invasive, and migratory capacities of HCC cells *in vitro*. Furthermore, it induced a pronounced boost in glycolysis, evidenced by increased levels of glucose uptake, lactate secretion, ECAR, and intracellular ATP. This rewiring of cellular metabolism toward glycolytic flux is a hallmark of cancer cells, known as the Warburg effect (Fukushi et al., 2022), which enables them to meet the heightened energetic and anabolic demands associated with uncontrolled growth. In this study, miR-500a-3p significantly enhanced the glycolytic ca-

pacity of HCC cells, providing sufficient ATP and biosynthetic precursors for rapid tumor cell growth. Glycolytic intermediates can fuel nucleotide synthesis via the pentose phosphate pathway, thereby supporting rapid proliferation (Zhang et al., 2023a). We found that miR-500a-3p concurrently suppresses apoptosis by elevating Bcl-2 and reducing Bax expression and the Cleaved-caspase3/caspase3 ratio. As Bcl-2 inhibits cytochrome c release and caspase activation, its upregulation potently blocks apoptosis (Qian et al., 2022). Thus, miR-500a-3p exerts a multi-dimensional oncogenic role by coordinately enhancing proliferation, glycolysis, and survival. Importantly, *in vivo* studies corroborated these findings, showing miR-500a-3p promoted tumor growth, increased Ki67, reduced apoptosis, downregulated SOCS2, and activated JAK2/STAT5 signaling. Together, these results validate the miR-500a-3p/SOCS2/JAK2/STAT5 axis as a key regulator of HCC progression and a promising therapeutic target.

Conclusion

The present work establishes miR-500a-3p as a key oncogenic driver in HCC through its regulation of SOCS2 and the JAK2/STAT5 axis. By inhibiting SOCS2, miR-500a-3p activates JAK2/STAT5 signaling, thereby stimulating proliferation, glycolysis, and cell survival. These findings contribute significantly to the understanding of HCC biology and suggest novel avenues for diagnosis and treatment. Subsequent research efforts could prioritize the clinical validation of miR-500a-3p, particularly its application as a circulating biomarker for early HCC detection and risk stratification. Meanwhile, targeted therapeutic strategies against miR-500a-3p, SOCS2, or the JAK2/STAT5 pathway, such as the combined use of miRNA inhibitors, SOCS2 agonists, or JAK2/STAT5 inhibitors, are expected to offer more effective treatment options for HCC patients. In addition, in-depth studies of the specific regulatory networks of miR-500a-3p in HCC metabolic reprogramming and its interactions with the tumor microenvironment will contribute to a comprehensive understanding of its oncogenic mechanisms and lay the foundation for developing more precise therapeutic strategies for HCC.

Ethical aspects and conflict of interest

The authors confirm that no generative artificial intelligence tools were used in the preparation of this manuscript and have no conflict of interest to declare.

References

Ally A, Balasundaram M, Carlsen R, Chuah E, Clarke A, Dhalla N, et al. (2017). Comprehensive and integrative genomic characterization of hepatocellular carcinoma. Cell 169(7): 1327–1341.e1323. DOI: 10.1016/j.cell.2017.05.046.

Amjad E, Pezzani R, Sokouti B (2024). A review of the literature on the use of CRISPR/Cas9 gene therapy to treat hepatocellular carcinoma. Oncol Res 32(3): 439–461. DOI: 10.32604/or.2023.044473.

Aziz F, Chakraborty A, Khan I, Monts J (2022). Relevance of miR-223 as Potential Diagnostic and Prognostic Markers in Cancer. Biology (Basel). 11(2): 249. DOI: 10.3390/biology11020249.

Baldini C, Moriconi FR, Galimberti S, Libby P, De Caterina R (2021). The JAK–STAT pathway: an emerging target for cardiovascular disease in rheumatoid arthritis and myeloproliferative neoplasms. Eur Heart J 42(42): 4389–4400. DOI: 10.1093/eurheartj/ehab447.

Cabrera-Galván JJ, Araujo E, de Mirecki-Garrido M, Pérez-Rodríguez D, Guerra B, Aranda-Tavío J, et al. (2023). SOCS2 protects against chemical-induced hepatocellular carcinoma progression by modulating inflammation and cell proliferation in the liver. Biomed Pharmacother 157: 114060. DOI: 10.1016/j.biopha.2022.114060.

Chandrashekar DS, Bashel B, Balasubramanya SAH, Creighton CJ, Ponce-Rodriguez I, Chakravarthi BVSK, Varambally S (2017). UALCAN: a portal for facilitating tumor subgroup gene expression and survival analyses. Neoplasia 19(8): 649–658. DOI: 10.1016/j.neo.2017.05.002.

Chandrashekar DS, Karthikeyan SK, Korla PK, Patel H, Shovon AR, Athar M, et al. (2022). UALCAN: An update to the integrated cancer data analysis platform. Neoplasia 25: 18–27. DOI: 10.1016/j.neo.2022.01.001.

Chen LL, Kim VN (2024). Small and long non-coding RNAs: Past, present, and future. Cell 187(23): 6451–6485. DOI: 10.1016/j.cell.2024.10.024.

Chen X, Wang Z, Zhao X, Zhang L, Zhou L, Li X, et al. (2022). STAT5A modulates CDYL2/SLC7A6 pathway to inhibit the proliferation and invasion of hepatocellular carcinoma by targeting to mTORC1. Oncogene 41(17): 2492–2504. DOI: 10.1038/s41388-022-02273-2.

Chen Y, Wang X (2020). miRDB: an online database for prediction of functional microRNA targets. Nucleic Acids Res 48(D1): D127–D131. DOI: 10.1093/nar/gkz757.

Cong P, Hou HY, Wei W, Zhou Y, Yu XM (2020). MiR-920 and LSP1 co-regulate the growth and migration of glioblastoma cells by modulation of JAK2/STAT5 pathway. J Bioenerg Biomembr 52(5): 311–320. DOI: 10.1007/s10863-020-09848-2.

Craig AJ, Von Felden J, Garcia-Lezana T, Sarcognato S, Villanueva A (2020). Tumour evolution in hepatocellular carcinoma. Nat Rev Gastroenterol Hepatol 17(3): 139–152. DOI: 10.1038/s41575-019-0229-4.

Eldosoky MA, Hammad R, Elmadbouly AA, Aglan RB, Abdel-Hamid SG, Alboraie M, et al. (2023). Diagnostic significance of hsa-miR-21-5p, hsa-miR-192-5p, hsa-miR-155-5p, hsa-miR-199a-5p panel and ratios in hepatocellular carcinoma on top of liver cirrhosis in HCV-infected patients. Int J Mol Sci 24(4): 3157. DOI: 10.3390/ijms24043157.

Fromm B, Billipp T, Peck LE, Johansen M, Tarver JE, King BL, et al. (2015). A Uniform System for the Annotation of Vertebrate microRNA Genes and the Evolution of the Human microRNAome. Annu Rev Genet 49: 213–242. DOI: 10.1146/annurev-genet-120213-092023.

Fukushi A, Kim HD, Chang YC, Kim CH (2022). Revisited metabolic control and reprogramming cancers by means of the Warburg effect in tumor cells. Int J Mol Sci 23(17): 10037. DOI: 10.3390/ijms231710037.

Ghasemian A, Omear HA, Mansoori Y, Mansouri P, Deng X, Darbeheshti F, et al. (2023). Long non-coding RNAs and JAK/STAT signaling pathway regulation in colorectal cancer development. Front Genet 14: 1297093. DOI: 10.3389/fgene.2023.1297093.

Guo H, Zhang C, Tang X, Zhang T, Liu Y, Yu H, et al. (2022). HHLA2 activates the JAK/STAT signaling pathway by binding to TMIGD2 in hepatocellular carcinoma cells. Inflammation 45(4): 1585–1599. DOI: 10.1007/s10753-022-01644-x.

Gutiérrez-Hoya A, Soto-Cruz I (2020). Role of the JAK/STAT pathway in cervical cancer: its relationship with HPV E6/E7 oncoproteins. Cells 9(10): 2297. DOI: 10.3390/cells9102297.

Guvenir Celik E, Eroglu O (2023). Combined treatment with ruxolitinib and MK-2206 inhibits the JAK2/STAT5 and PI3K/AKT pathways via apoptosis in MDA-MB-231 breast cancer cell line. Mol Biol Rep 50(1): 319–329. DOI: 10.1007/s11033-022-08034-4.

He M, Cai Y, Yuan Z, Zhang L, Lu H (2023). Upregulation of SOCS2 causes mitochondrial dysfunction and promotes ferroptosis in pancreatic cancer cells. Acta Biochim Pol 70(1): 163–168. DOI: 10.18388/abp.2020_6383.

Heath AP, Ferretti V, Agrawal S, An M, Angelakos JC, Arya R, et al. (2021). The NCI genomic data commons. Nat Genet 53(3): 257–262. DOI: 10.1038/s41588-021-00791-5.

Hu X, Li J, Fu M, Zhao X, Wang W (2021). The JAK/STAT signaling pathway: from bench to clinic. Signal Transduct Target Ther 6(1): 402. DOI: 10.1038/s41392-021-00791-1.

Huang IH, Chung WH, Wu PC, Chen CB (2022). JAK-STAT signaling pathway in the pathogenesis of atopic dermatitis: An updated review. Front Immunol 13: 1068260. DOI: 10.3389/fimmu.2022.1068260.

Ito T, Nguyen MH (2023). Perspectives on the underlying etiology of HCC and its effects on treatment outcomes. J Hepatocell Carcinoma 10: 413–428. DOI: 10.2147/JHC.S347959.

Jiang C, Long J, Liu B, Xu M, Wang W, Xie X, et al. (2017). miR-500a-3p promotes cancer stem cells properties via STAT3 pathway in human hepatocellular carcinoma. J Exp Clin Cancer Res 36(1): 99. DOI: 10.1186/s13046-017-0568-3.

Jiang M, Fang H, Tian H (2025). Metabolism of cancer cells and immune cells in the initiation, progression, and metastasis of cancer. Theranostics 15(1): 155–188. DOI: 10.7150/thno.103376.

Juaid N, Amin A, Abdalla A, Reese K, Alamri Z, Moulay M, et al. (2021). Anti-hepatocellular carcinoma biomolecules: molecular targets insights. Int J Mol Sci 22(19): 10774. DOI: 10.3390/ijms221910774.

Keewan E, Matlawska-Wasowska K (2021). The emerging role of suppressors of cytokine signaling (SOCS) in the development and progression of leukemia. Cancers 13(16): 4000. DOI: 10.3390/cancers13164000.

Khare S, Khare T, Ramanathan R, Ibdah JA (2022). Hepatocellular carcinoma: the role of MicroRNAs. Biomolecules 12(5): 645. DOI: 10.3390/biom12050645.

Kim YS, Park SJ, Lee YS, Kong HK, Park JH (2016). miRNAs involved in LY6K and estrogen receptor α contribute to tamoxifen-susceptibility in breast cancer. Oncotarget 7(27): 42261–4273. DOI: 10.18632/oncotarget.9950.

Kopalli SR, Annamneedi VP, Koppula S (2022). Potential natural biomolecules targeting JAK/STAT/SOCS signaling in the management of atopic dermatitis. Molecules 27(14): 4660. DOI: 10.3390/molecules27144660.

Kouroumalis E, Tsomidis I, Voumvouraki A (2023). Pathogenesis of hepatocellular carcinoma: the interplay of apoptosis and autophagy. Biomedicines 11(4): 1166. DOI: 10.3390/biomedicines11041166.

Letellier E, Haan S (2016). SOCS2: physiological and pathological functions. Front Biosci (Elite Ed) 8(1): 189–204. DOI: 10.2741/E760.

Li L, Xiao C, He K, Xiang G (2021). Circ_0072088 promotes progression of hepatocellular carcinoma by activating JAK2/STAT3 signaling pathway via miR-375. IUBMB Life 73(9): 1153–1165. DOI: 10.1002/iub.2520.

Liao X, Xie Z, Guan C (2018). MiRNA-500a-3p inhibits cell proliferation and invasion by targeting lymphocyte antigen 6 complex locus K (LY6K) in human non-small cell lung cancer. Neoplasma 65(5): 673–682. DOI: 10.4149/neo_2018_170516N355.

Liu G, Huang K, Lin B, Zhang R, Zhu Y, Dong X, et al. (2025). IKZF1 promotes pyroptosis and prevents M2 macrophage polarization by inhibiting JAK2/STAT5 pathway in colon cancer. Biochim Biophys Acta Mol Basis Dis 1871(3): 167690. DOI: 10.1016/j.bbadis.2025.167690.

Liu Y, Tang W, Ren L, Liu T, Yang M, Wei Y, et al. (2022). Activation of miR-500a-3p/CDK6 axis suppresses aerobic glycolysis and colorectal cancer progression. J Transl Med 20(1): 106. DOI: 10.1186/s12967-022-03308-8.

Long J, Liu B, Yao Z, Weng H, Li H, Jiang C, Fang S (2022). miR-500a-3p is a potential prognostic biomarker in hepatocellular carcinoma. Int J Gen Med 15: 1891–1899. DOI: 10.2147/IJGM.S340629.

Lv Y, Xie X, Zou G, Kong M, Yang J, Chen J, Xiang B (2023). SOCS2 inhibits hepatoblastoma metastasis via downregulation of the JAK2/STAT5 signal pathway. Sci Rep 13(1): 21814. DOI: 10.1038/s41598-023-48591-7.

McGeary SE, Lin KS, Shi CY, Pham TM, Bisaria N, Kelley GM, Bartel DP (2019). The biochemical basis of microRNA targeting efficacy. Science 366(6472): eaav1741. DOI: 10.1126/science.aav1741.

Pang J, Huang P, Huang H, Ma J, He L, Lin X, et al. (2025). Molecular mechanism and role of miRNA-155 ribonucleic acid in podocyte apoptosis in lupus nephritis: SOCS1 protein expression regulates JAK/STAT pathway transduction. Int J Biol Macromol 304(Pt 1): 140810. DOI: 10.1016/j.ijbiomac.2025.140810.

Park H, Lee S, Lee J, Moon H, Ro SW (2023). Exploring the JAK/STAT Signaling Pathway in Hepatocellular Carcinoma: Unraveling Signaling Complexity and Therapeutic Implications. Int J Mol Sci 24(18): 13764. DOI: 10.3390/ijms241813764.

Qian S, Wei Z, Yang W, Huang J, Yang Y, Wang J (2022). The role of BCL-2 family proteins in regulating apoptosis and cancer therapy. Front Oncol 12: 985363. DOI: 10.3389/fonc.2022.985363.

Rahbar Farzam O, Najafi S, Amini M, Rahimi Z, Dabbaghipour R, Zohdi O, et al. (2024). Interplay of miRNAs and lncRNAs in STAT3 signaling pathway in colorectal cancer progression. Cancer Cell Int 24(1): 16. DOI: 10.1186/s12935-023-03202-3.

Raymant M, Astuti Y, Alvaro-Espinosa L, Green D, Quaranta V, Bellomo G, et al. (2024). Macrophage-fibroblast JAK/STAT dependent crosstalk promotes liver metastatic outgrowth in pancreatic cancer. Nat Commun 15(1): 3593. DOI: 10.1038/s41467-024-47949-3.

Reda El Sayed S, Cristante J, Guyon L, Denis J, Chabre O, Cherradi N (2021). MicroRNA therapeutics in cancer: current advances and challenges. Cancers 13(11): 2680. DOI: 10.3390/cancers13112680.

Ren J (2024). Advances in Combination Therapy for Gastric Cancer: Integrating Targeted Agents and Immunotherapy. Adv Clin Pharmacol Ther 1(1): 1–15. DOI: 10.63623/9k14tf70.

Sangro B, Sarobe P, Hervás-Stubbs S, Melero I (2021). Advances in immunotherapy for hepatocellular carcinoma. Nat Rev Gastroenterol Hepatol 18: 525–543. DOI: 0.1038/s41575-021-00438-0.

Semina EV, Rysenkova KD, Troyanovskiy KE, Shmakova AA, Rubina KA (2021). MicroRNAs in cancer: from gene expression regulation to the metastatic niche reprogramming. Biochemistry (Moscow) 86(7): 785–799. DOI: 10.1134/S0006297921070014.

Shademan B, Karamad V, Nourazarian A, Avci CB (2025). Exploring microRNA targeting as a promising approach for solid tumor treatment. Front Oncol 15: 1570093. DOI: 10.3389/fonc.2025.1570093.

Shao F, Pang X, Baeg GH (2021). Targeting the JAK/STAT signaling pathway for breast cancer. Curr Med Chem 28(25): 5137–5151. DOI: 10.2174/0929867328666201207202012.

Sharma KK, Mohsin M, Mittal P, Ali Z, Fatma N, Upadhyay P, et al. (2024). Diagnosis of the initial stage of hepatocellular carcinoma: A review. Curr Pharm Des 30(22): 1708–1724. DOI: 10.2174/0113816128298875240321073907.

Shen Y, Zhao N, Zhao N, Hu X, He X, Xu Y, et al. (2022). Tumor-suppressive and oncogenic roles of microRNA-149-5p in human cancers. Int J Mol Sci 23(18): 10823. DOI: 10.3390/ijms231810823.

Shires KL, Rust AJ, Harryparsad R, Coburn JA, Gopie RE (2023). JAK2/STAT5 Pathway Mutation Frequencies in South African BCR/ABL Negative MPN Patients. Hematol Oncol Stem Cell Ther 16(3): 291–302. DOI: 10.56875/2589-0646.1064.

Sobah ML, Liongue C, Ward AC (2021). SOCS proteins in immunity, inflammatory diseases, and immune-related cancer. Front Med 8: 727987. DOI: 10.3389/fmed.2021.727987.

Sticht C, De La Torre C, Parveen A, Gretz N (2018). miRWalk: an online resource for prediction of microRNA binding sites. PloS One 13(10): e0206239. DOI: 10.1371/journal.pone.0206239.

Tang Z, Li C, Kang B, Gao G, Li C, Zhang Z (2017). GEPIA: a web server for cancer and normal gene expression profiling and interactive analyses. Nucleic Acids Res 45(W1): W98–W102. DOI: 10.1093/nar/gkx247.

Tong JL, Wang LL, Ling XF, Wang MX, Cao W, Liu YY (2019). MiR-875 can regulate the proliferation and apoptosis of non-small cell lung cancer cells via targeting SOCS2. Eur Rev Med Pharmacol Sci 23(12): 5235–5241. DOI: 10.26355/eurrev_201906_18189.

Tufail M, Jiang CH, Li N (2024). Altered metabolism in cancer: insights into energy pathways and therapeutic targets. Mol Cancer 23(1): 203. DOI: 10.1186/s12943-024-02119-3.

Valle-Mendiola A, Gutierrez-Hoya A, Soto-Cruz I (2023). JAK/STAT signaling and cervical cancer: from the cell surface to the nucleus. Genes 14(6): 1141. DOI: 10.3390/genes14061141.

Wang F, Wang X, Li J, Lv P, Han M, Li L, et al. (2021). CircNOL10 suppresses breast cancer progression by sponging miR-767-5p to regulate SOCS2/JAK/STAT signaling. J Biomed Sci 28(1): 4. DOI: 10.1186/s12929-020-00697-0.

Wang H, Zhang X, Li Y, Li Y, Pang T (2022). Lidocaine hampers colorectal cancer process via circITFG2/miR-1204/SOCS2 axis. Anticancer Drugs 33(3): 235–244. DOI: 10.1097/CAD.0000000000001091.

Xia C, Dong X, Li H, Cao M, Sun D, He S, et al. (2022). Cancer statistics in China and United States, 2022: profiles, trends, and determinants. Chin Med J 135(5): 584–590. DOI: 10.1097/CM9.0000000000002108.

Xiang Y, Zong QB, Liu H, Li HN, Wu QF, Dai ZT, et al. (2023). lncRNA IGF2-AS regulates miR-500a-3p/PPP4R1/p-VEGFR2 signalling pathway to promote thyroid carcinoma progression and tubulogenesis. Clin Transl Med 13(4): e1240. DOI: 10.1002/ctm2.1240.

Yan M, Sun Z, Zhang S, Yang G, Jiang X, Wang G, et al. (2024). SOCS modulates JAK-STAT pathway as a novel target to mediate the occurrence of neuroinflammation: Molecular details and treatment options. Brain Res Bull 213: 110988. DOI: 10.1016/j.brainresbull.2024.110988.

Yousefnia S (2022). A comprehensive review on miR-153: mechanistic and controversial roles of miR-153 in tumorigenicity of cancer cells. Front Oncol 12: 985897. DOI: 10.3389/fonc.2022.985897.

Zhang F, Wu Z, Yu B, Ning Z, Lu Z, Li L, et al. (2023a). ATP13A2 activates the pentose phosphate pathway to promote colorectal cancer growth though TFEB-PGD axis. Clin Transl Med 13(5): e1272. DOI: 10.1002/ctm2.1272.

Zhang H, Li S, Wang D, Liu S, Xiao T, Gu W, et al. (2024). Metabolic reprogramming and immune evasion: the interplay in the tumor microenvironment. Biomark Res 12(1): 96. DOI: 10.1186/s40364-024-00646-1.

Zhang W, Xie Y, Yu X, Liu C, Gao W, Xing W, Si T (2023b). ABHD17C, a metabolic and immune-related gene signature, predicts prognosis and anti-PD1 therapy response in pancreatic cancer. Discov Oncol 14(1): 87. DOI: 10.1007/s12672-023-00690-7.

Zhang Y, Li X, Chen H, Li J, Guo X, Fang Y, et al. (2025). Cancer Cell-Derived Exosomal miR-500a-3p Modulates Hepatic Stellate Cell Activation and the Immunosuppressive Microenvironment. Adv Sci (Weinh) 12(2): e2404089. DOI: 10.1002/advs.202404089.

Zhang Y, Wang S, Han S, Feng Y (2022). Pan-cancer analysis based on EPOR expression with potential value in prognosis and tumor immunity in 33 tumors. Front Oncol 12: 844794. DOI: 10.3389/fonc.2022.844794.

Zhou J, Tison K, Zhou H, Bai L, Acharyya RK, McEachern D, et al. (2025). STAT5 and STAT3 balance shapes dendritic cell function and tumour immunity. Nature 643(8071): 519–528. DOI: 10.1038/s41586-025-09000-3.

Zhou XH, Xu H, Xu C, Yan YC, Zhang LS, Sun Q, et al. (2022). Hepatocellular carcinoma-derived exosomal miRNA-761 regulates the tumor microenvironment by targeting the SOCS2/JAK2/STAT3 pathway. World J Emerg Med 13(5): 379–385. DOI: 10.5847/wjem.j.1920-8642.2022.089.

Zhu Y, Yang Y, Lan Y, Yang Z, Gao X, Zhou J (2025). The role of PKM2-mediated metabolic reprogramming in the osteogenic differentiation of BMSCs under diabetic periodontitis conditions. Stem Cell Res Ther 16(1): 186. DOI: 10.1186/s13287-025-04301-w.